Vol.7 No.1 Jan 2024

Journal of Computational Mechanics, Power System and Control

Received 13 October, Revised 2 December, Accepted 17 January

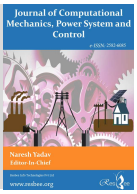

Insight Into the Fluid Flow Through the Porous Medium Between Two Vertical Walls Due to Buoyancy Forces, Convectively Heating of Left Wall, Space-Dependent Heat Source But Subject to Lorentz Force

Muhammed Murtala Hamza
UsmanuDanfodiyo University, P.M.B. 2346, Sokoto, Nigeria

Abdulsalam Shuaibu
The Federal University of Agriculture Zuru, P.M.B 28, Kebbi State, Nigeria.

Ahmad Samaila Kamba
Usmanu Danfodiyo University, P.M.B. 2346, Sokoto, Nigeria

Godwin Ojemeri
The Federal University of Agriculture Zuru, P.M.B 28, Kebbi State, Nigeria

Abstract: The area of fluid dynamics known as magnetohydrodynamics (MHD) studies how magnetic fields affect fluid flow. Its existence in a variety of geometries has become an enthralling aspect of science and technology. Cooling nuclear reactors and medical research are all practical uses. In the current work, we investigate free convective slip flow between two vertical walls generated by convective heating of the left wall in steady and unsteady state magnetohydrodynamics with chemical kinetic exponents. In general, we present two sets of solutions: a constant state and a transient state. The implicit finite difference method and the homotopy perturbation approach were used to obtain the two solutions. Line graphs were utilized to depict the effects of various flow factors included in the system.The findings demonstrated that a slight rise in MHDdecreases the momentum barrier layer by inducing the Lorentz force.However, slows the flow and depictsthe best view at the biomolecular chemical reaction index. Furthermore, it was demonstrated that in contrast to Arrhenius and Sensitized, higher fluid velocity and temperature at biomolecular chemical processes result in significant increases in temperature and velocity gradients, while fluid velocity is found to be significantly improved with a slight increase in a porous medium. Significant agreement can also be seen when comparing the steady state and the unsteady solution.

Keywords: Convectively heating; Chemical Kinetic exponent; MHD; Porous Medium; Navier slip

Nomenclature

Abbreviation	Expansion
MHD	Magne to Hydro Dynamics

1. Introduction

MHD is a unique area of fluid dynamics where magnetic fields play a significant role in fluid movement. Its presence in many geometries has become an intriguing part of science and technology. It has practical applications in the earth's magnetic field, fusion, solar wind and flares, and medical research. Chemodynamics, a study that examines chemical reactions in particular their rates, pathways, and structures, is the name given to chemical processes that concentrate on cogeneration-related reactions. There are three categories of chemical kinetic exponents (m): Arrhenius, sensitized, and biomolecular processes. A detailed grasp of aerodynamics, mass and heat transfer, and reaction kinetics is necessary for studying chemical processes.

The main objective of the chemical reaction process is to optimize the chemical reaction, solvent composition, and operational parameters. Concepts of chemical reactions were created mainly for the petrochemical sector. In biologically related fields and technologies, such as biotechnology, biochemicals, bio energy, nutrition, and other systems based on similar ideas, chemical species communication and transport are important. Modern mathematical models are increasingly being used to improve convective heat transfer by including porous media. Using porous material in a cutting-edge mathematical model to enhance heat transfer is becoming more popular. In a variety of situations, porous media channels are commonly employed to transfer and transmit fluids and heat, including design, building construction, humidity, and moisture, as well as passive cooling, ultra filtration, geothermal recovery, and oil exploration. This method proved that Higher fluid velocity and temperature at bio molecular chemical

https://doi.org/10.46253/jcmps.v7i1.a5

processes result in significant increases in temperature and velocity gradients, while fluid velocity is significantly improved with a slight increase in a porous medium.

The paper is organized as follows: Section 2 covers the literature review. Section 3 details the problem formulation, and 4 emphasizes the technique for solving. Section 5 mentions the Numerical solution. Section 6 mentions the discussion of the findings. Section 6 explains the advantages and disadvantages and section 7 concludes the paper.

2. Literature review

Many research has been undertaken to study the effects of viscous reactions. On combined convection embedded with a porous medium and continuous heat flow on the vertical plate, [1] offered numerous uses of porous media in science and technology. The author [2] asserts that porous medium heat exchangers and channels are an alternative during mixed convection in porous media adjacent to a vertical uniform heat flux surface on applying Hamming's predictor-corrector method.[3] expanded the boundary layer issue to incorporate spontaneous convection flow in embedded porous material around an isothermal sphere. Mahmoodi and colleagues [4] concluded that a porous medium has a substantial impact on fluid production and proposed a solid matrix made up of pores and vacuum spaces that let fluid pass through and are connected by a network of channels. An alternative study was also conducted on unsteady MHD free convective flow in a vertical tube covered with absorbent material [5].Porous media are sometimes employed in a unique computational framework to increase convective heat transfer properties for some utilizations, including radioactive waste storage, transpiration cooling, crude oil refining, and building heating and cooling. Hamza and colleagues [6] investigated MHD-free convection flow in a vertical plate embedded with porous material. They identified that porous media had a major impact on fluid flow. Wakif [7], who used the generalized Buongiorno's nanofluid model to investigate the effects of thermal emission and surface roughness on the thermo-magneto-hydrodynamic stability of alumina-copper oxide hybrid nanofluids, concluded that as the Lorentz force, thermal radiation, and surface roughness increased in strength, they had a more substantial stabilizing effect on the appearance of convection cells. The Lorentz force plays a significant role in temperature distribution, but on the other hand, the heat transfer rate decreases with increasing values of the Lorentz force. Shawky [8] looked into the stretching sheet issue in a porous medium when a magnetic field was present. In addition to looking into the flow of three-dimensional boundary layers. Cortell [9] also looks into the flow through porous media and a vertical stretching sheet considering two-dimensional boundary layers. Nadeem *et al.* [10] used a three-dimensional Casson fluid flow across an absorbent material sheet. The effect of radiant heat on MHD flow is examined by Harshad [11] using the heat and mass transfer of micropolar fluid over two vertical walls. Concluding that MHD, mixed convection, and buoyancy are responsible for the improvement of the velocity profile, [12] analyzes the impacts of cross-diffusion and heat production on mixed convection stagnation points of MHD cartesian fluid in a porous media.

Jat *et al.* [13] recently examined viscous fluid's MHD boundary layer flow through a nonlinearly stretched sheet buried in a porous media. The work by Khalid *et al.* [14] on Casson fluid flow over an oscillating plate submerged in a porous medium was elaborated upon in this. They noticed that increasing the porosity parameter decreased velocity, which led to an increase in the skin friction coefficient. These assessments did not consider the potential for a slide scenario close to the wall. In some physical circumstances, preventing incurring velocity loss near the border is hard. In the case of non-Newtonian fluids, in particular, a slip condition at the wall is required. For instance, the velocity slip near the wall of the softening plastic is constant. Fluids with a slip state at the chamber wall can be used to sharpen artificial heart valves and cavities within the body. Investigating the boundary layer's convective boundary condition is necessary to comprehend fluid boundary layer flow, both Newtonian and non-Newtonian. Due to its practical usage in several sectors and real-world applications, the majority of research is therefore concentrated on maintaining wall temperature and heat flow rate stability. For instance, convection flows in the water pipes to cool automobile engines, and water is a great conductor of heat away from the engine to the radiator. To enable the formation of convection currents, air conditioners are mounted close to the room's ceiling. The room is filled with chilly, dry air thanks to the air conditioner. Cool air sinks because it is denser. Due to its lower density, heated air will ascend. The temperature of the air will ultimately drop to the correct level due to air circulation. The results of the research in [15], [16], [17], and [18] serve as prerequisites. The effect of heat radiation on the flow of a viscous fluid boundary layer within a moving plate in the presence of a moving plate subjected to a convective boundary condition was then investigated by Ishak et al. [19].

When internal resistance is much lower than surface resistance, a process known as convective heating. Due to multiple uses, including heat exchangers, conjugate heat transfer around fins, the petroleum sector, and solar radiation, this type of fluid flow has attracted much interest. In an originated

work, Kurma [20] scrutinized the Radiation effect on MHD grooves with magnetic field stimulation and Newtonian heating/cooling. However, he ascertained that numerical skin friction and Nusselt number optimize for a rise in Newtonian heating while the reverse mechanism is demonstrated for Newtonian cooling. Numerical research on the Newtonian heating impact on heat-absorbing MHD Cascason flow of dissipative fluid via an oscillating vertical porous plate was recently suggested by Reddy and Sademaki [21]. MHD flow with Newtonian heating and cooling and an induced magnetic field have been analytically investigated by Kumar and Singh [22]. Numerous scholars study various facets of joule heating and Newtonian heating flow transfer phenomena using MHD. The papers [23], and [24] are recommended to interested authors for more information. The impact of radiation, heat source/sink, and Newtonian heating has been studied by Gangadhar *et al.* [25]. Chamkha [26] states that a rotating vertical porous channel submerged in a Darcian porous regime exhibits Hartmann-Newtonian radiating MHD flow. Hamza [27] examined the impact of convective heating and momentum navigator slip on an exothermic fluid's spontaneous convection flow between vertical channels. Exothermic fluid between vertical channels was examined similarly in Hamza's most recent study [28].

The mechanisms of convective boundary conditions for the three-dimensional hydromagnetic flow were demonstrated by Mahanta and Shaw [29]. According to Hamza and Abdulsalam [30], several well-known chemical reactions occur in industrial environments, including exothermal and isothermal. Examples include isothermal and exothermal reactions. Many studies into chemical reactions and their phenomena have been done recently. Examples include the effects of enzyme activity on heat conduction and the effects of mass moving on boundary surfaces under different boundary and starting conditions. Saeed and colleagues [31] used free convection, an enzymatic process, and a wall slip boundary condition to study heat conduction and mass transfer in a closed system. The fluid flow phenomena connected to the two different boundary conditions—slip and no-slip boundary conditions—are described by Jan and colleagues [32]. The initial layer of fluid momentum hitting the plate's surface has a velocity proportional to the plate's speed or boundary under no-slip boundary circumstances. It may be advantageous for the slip boundary condition to affect nano- and micro-channels. In both the manufacturing sector and the chemical sciences, slip conditions are crucial. Bestman [33], Alabraba, *et al.* [34], and Hamza *et al* [35] considered the Arrhenius activation energy when developing their configurations. This study looks at the free convective slip flow's transient and steady-state MHD chemical kinetic exponent in a vertical channel-filled porous medium. The steady-state analytical solution was addressed with the homotopy perturbation method using the fundamental equations of momentum, energy, and related boundary conditions in dimensionless form. An implicit finite difference scheme approach is used in the scenario of the transient state.

3. Problem formulation

A time-dependent flow in a vertical channel with a porous material was considered with distance H. The fluid's reaction and the bottom channel's constant temperature produce the flow. As a result, the inside surface of the channel kept its overall surface thickness and temperature constant. In areas with a porous material, there is natural heat transmission. The temperature increased from the center outward.

In Fig. 1, the flow creation is shown. Hamza [27] describes a non-dimensional set of equations under Boussinesq's premise. The following is a presumption we make:

1. The transverse magnetic field has a significant effect in contrast to the buoyancy force.
2. The lower channel's Newtonian heating of the plate is taken into account
3. Chemical reaction parameters and the chemical kinetic exponent are also considered.
4. Joule heating's effects are disregarded.

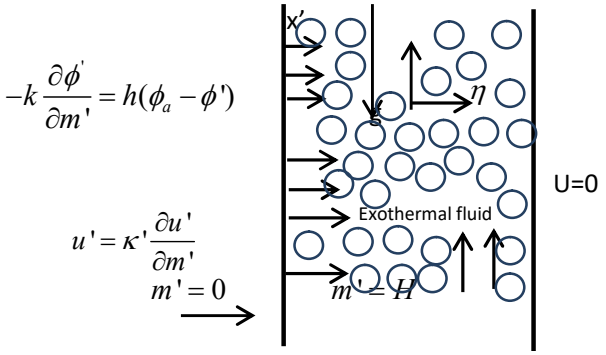

Fig. 1. *Framework of physical flow*

Governing equation in Dimensional form

$$\frac{\partial u'}{\partial t'} = \nu \frac{\partial^2 u'}{\partial m'^2} - \frac{\sigma B_o y_o^2}{\rho \nu} u' - \left(\frac{1}{k}\right) u' + g\beta\left(T' - T_o'\right) \tag{1}$$

$$\frac{\partial \phi'}{\partial t'} = \frac{k}{pC_p} \frac{\partial^2 \phi'}{\partial m'^2} + QC_0 A \left(\frac{KT}{VL}\right)^m e^{\left(\frac{-E}{R\phi'}\right)} \tag{2}$$

The starting point and boundary conditions for the current investigation are as follows:

$$\left.\begin{aligned} & t' \le 0 : u'0, \quad \phi' \to \phi'_0, \; 0 \le m' \le H \\ & t'0 : u' = \kappa^* \frac{\partial u'}{\partial m'}, \quad -k \frac{\partial \phi'}{\partial m'} - h[\phi'_0 - \phi'] = 0, \; at \; m' = 0 \\ & u' = 0, \quad \phi' = \phi'_0, \; as \quad m' \to H \end{aligned}\right\} \tag{3}$$

$$\left.\begin{aligned} & m = \frac{m'}{H}, \; t = \frac{t'\mu_0}{H^2}, \; \phi = \frac{E(\theta' - \theta_0)}{R\theta_0^2}, \; \varepsilon = \frac{R\theta_0}{E}, \; U = \frac{u'\mu_0 E}{g\beta H^2 R\phi_0^2}, \; Gr = \frac{g\beta(\phi_1 - \phi_0)}{\nu^2} \\ & \lambda = \left(\frac{K\phi_0}{vl}\right)^m \frac{QC_0 AEH^2}{R\phi_0^2} e^{\left(\frac{-E}{R\phi_0}\right)}, \; \mathrm{Pr} = \frac{\mu_0 pC_p}{k}, \; \kappa = \frac{\kappa^*}{H}, \; \phi_a = \frac{E(\theta_a - \theta_0)}{R\theta_0^2}, \; Bh = \frac{hH}{k}, \\ & Da = \frac{k_0}{b^2}, \; Ha^2 = \frac{\sigma B_0^2 r_0^2}{\rho \nu} \end{aligned}\right\} \tag{4}$$

Substituting (4), into (1)-(3), the governing equation becomes

$$\frac{\partial u}{\partial t} = \frac{\partial^2 u}{\partial m^2} - \left(H^2 a + \frac{1}{Da}\right) u + \phi \tag{5}$$

$$\mathrm{Pr} \frac{\partial^2 \phi}{\partial t} = \frac{\partial^2 \phi}{\partial m^2} + \lambda (1 + \varepsilon\phi)^m e^{\frac{\phi}{1+\varepsilon\phi}} \tag{6}$$

The non-dimensional boundary condition is given as

$$\left.\begin{aligned} & U = 0, \; \phi = 0, \quad 0 \le m \le 1, \qquad t \le 0 \\ & t > 0 : U = \kappa \frac{\partial u}{\partial m}, \quad \frac{\partial \phi}{\partial m} = Bh[\phi - \phi_a], \; at \; m = 0 \\ & U = 0, \quad \phi = 0, \; as \quad m = 1 \end{aligned}\right\} \tag{7}$$

Steady State

$$\frac{d^2 U}{dm^2} - \left(H^2 a + \frac{1}{Da}\right) U + \phi = 0 \tag{8}$$

$$\frac{d^2 \phi}{dm^2} + \lambda (1 + \varepsilon\phi)^m e^{\left(\frac{\phi}{1+\varepsilon\phi}\right)} = 0 \tag{9}$$

fluid-wall boundary condition is:

$$\left.\begin{aligned} & U - \kappa \frac{dU}{dm} = 0, \quad \frac{d\phi}{dm} - Bh[\phi - \phi_a] = 0, \qquad at \qquad m = 0 \\ & U = 0, \qquad \phi = 0, \qquad at \qquad m = 1 \end{aligned}\right\} \tag{10}$$

4. Technique for solving

We use the Homotopy perturbation approach on equations (8) and (9). Then we have:

$$H(U, p) = (1 - p) \frac{d^2 U}{dm^2} - p\left[\left(H^2 a + \frac{1}{Da}\right) U - \phi\right] \tag{11}$$

$$H(T, p) = (1 - p) \frac{d^2 \phi}{dm^2} + p\left[\lambda(1 + m\varepsilon)\phi + (\frac{1}{2} + (m-1)\varepsilon + \frac{m}{2}(m-1)\varepsilon^2)\phi^2\right] \tag{12}$$

We construct Homotopy on equations (8) and (9) and assume the solution to be in the form of

$$\left.\begin{aligned} & T(m) = \phi_0 + p\phi_1 + p^2\phi_2 + \ldots \\ & U(m) = u_0 + pu_1 + p^2 u_2 + \ldots \end{aligned}\right\} \tag{13}$$

Substituting (13) into (8) and (9) and comparing the coefficient of like power p, we get the following sets of differential equations.

$$p^0:\begin{cases}\dfrac{d^2\phi_0}{dm^2}=0\\ \dfrac{d^2u_0}{dm^2}=0\end{cases} \qquad \text{(14) and (15)}$$

The boundary conditions have now become.

$$\left.\begin{aligned}&\frac{d\phi_0}{dm}-Bh[\phi_0-\phi_a]=0\\ &u_0-\kappa\frac{du_0}{dm}=0\end{aligned}\right\}at\quad m=0 \qquad (16)$$

$$\left.\begin{aligned}&T_0=0\\ &u_0=0\end{aligned}\right\}\quad at\quad m=1 \qquad (17)$$

$$p^1:\begin{cases}\dfrac{d^2\phi_1}{dm^2}+\lambda(1+D_1\phi_0+\dfrac{1}{2}\phi_0^2+D_2\phi_0^2+D_3\phi_0^2)=0\\ \dfrac{d^2u_1}{dm^2}-\left(H^2a+\dfrac{1}{Da}\right)u_0+\phi_0=0\end{cases} \qquad \text{(18) and (19)}$$

Where

$$D_1=(1+m\varepsilon),\ \ D_2=(m-1)\varepsilon,\ \ D_3=\frac{m}{2}(m-1)\varepsilon^2, R=\left(H^2a+\frac{1}{Da}\right)$$

Fluid boundary conditions now become

$$\left.\begin{aligned}&\frac{d\phi_1}{dm}=Bh[\phi_1]\\ &u_1=\kappa\frac{du_1}{dm}\end{aligned}\right\}at\quad m=0 \qquad (20)$$

$$\left.\begin{aligned}&\phi_1=0\\ &u_1=0\end{aligned}\right\}at\quad m=1 \qquad (21)$$

$$p^2:\begin{cases}\dfrac{d^2\phi_2}{dm^2}+\lambda(D_1\phi_1+\phi_1\phi_0+2D_2\phi_1\phi_0+2D_3\phi_1\phi_0)=0\\ \dfrac{d^2u_2}{d\phi^2}-\left(H^2a+\dfrac{1}{Da}\right)u_1+\phi_1=0\end{cases} \qquad \text{(22) and (23)}$$

The fluid wall conditions now become

$$\left.\begin{aligned}&\frac{d\phi_2}{dm}=Bh[\phi_2]\\ &u_2=\kappa\frac{du_2}{dm}\end{aligned}\right\}\quad at\quad m=0 \qquad (24)$$

$$\left.\begin{aligned}&\phi_2=0\\ &u_2=0\end{aligned}\right\}\quad at\quad m=1 \qquad (25)$$

Setting p=1, the solutions of the differential equations in the approximate form becomes

$$\left.\begin{aligned}&\phi=\lim_{p\to1}\phi=\phi_0+\phi_1+\phi_2+\ldots\\ &U=\lim_{p\to1}U=u_0+u_1+u_2+\ldots\end{aligned}\right\} \qquad (26)$$

The series (13) usually converges, even for a few terms. On the other hand, the nonlinear operator controls the pace of convergence. Only a few terms of the H.P.M. series may be utilized to approximate the answer since the series solution converges through homotopy perturbation.

The solutions $\phi_0,\phi_1,\phi_2\cdots$ and $u_0,u_1,u_2\cdots$ are as follows:

$$\phi_0=v_0m+v_1 \qquad (27)$$

$$\phi_1=-\lambda\left\{\frac{m^2}{2}+D_1D_4+D_5+D_2D_6+D_3D_7\right\}+v_2m+v_3 \qquad (28)$$

$$u_1 = -\left[\ v_0 \frac{m^3}{6} + v_1 \frac{m^2}{2}\ \right] + v_7 m + v_8 \tag{29}$$

$$u_2 = R(-D_8 + D_9 + D_{10}) - \{-\lambda(D_{11} + D_1 D_{12} + D_{13} + D_2 D_{14} + D_3 D_{15}) + D_{16}\} + v_9 m + v_{10} \tag{30}$$

The stress distribution and heat transfer rate across both plates are givenby:

$$Nu_0 \Leftrightarrow \left.\frac{d\phi}{dm}\right|_{m=0} = v_0 + v_2 \tag{31}$$

$$Nu_1 \Leftrightarrow \left.\frac{d\phi}{dm}\right|_{m=1} = v_0 - \lambda\left[1 + D_1 L_7 + L_8 + D_2 L_9 + D_3 L_{10}\right] + v_2 \tag{32}$$

$$Sk_0 \Leftrightarrow \left.\frac{du}{dm}\right|_{m=0} = v_7 + v_9 \tag{33}$$

$$Sk_1 \Leftrightarrow \left.\frac{du}{dm}\right|_{m=1} = -L_1 + v_7 + R\left(-L_2 + \frac{v_7}{2} + v_8\right) - \left(-\lambda(\frac{1}{6} + D_1 L_3 + L_4 + D_2 L_5 + D_3 L_6) + \frac{v_2}{2} + v_3\right) + v_9 \tag{34}$$

5. Numerical solution

The partial differential equations (5) and (6) were solved by a numerical method known as the implicit finite difference method using boundary conditions (7). All time differentials were calculated using the forward difference formula, and second-order central differences were utilized to approximate the first and second derivatives. The final nodes are changed to take into consideration the model parameters while the equations represent the initial components. The following is a description of the I.F.D. equation for settings (5) and (6):

$$-rU_{i-1}^{j-1} + (1+2r)U_i^{j+1} - rU_{i+1}^{j+1} = (1-M^2)U_i^j + [1 - M^2\Delta t - \frac{1}{Da}\Delta t]U_i^j \tag{35}$$

$$-r\phi_{i-1}^{j+1} + (\mathrm{Pr}+2r)\phi_i^{j+1} - r\phi_{i+1}^{j+1} = \mathrm{Pr}\,\phi_i^j + \lambda(1\varepsilon\phi_i^j)^m \Delta t \exp\left(\frac{\phi_i^j}{1+\varepsilon\phi_i^j}\right) \tag{36}$$

6. Discussion of the findings

The following default values are used in the computation:
$\lambda = 0.1,\ Bh = 0.1,\ \phi_a = 1,\ \varepsilon = 1,\ m = 0.5,\ k = 0.1,\ M = 2,\ Da = 0.1$

6. 1 Transient and Steady-state Profile

We provide the transient solutions for velocity and temperature in Figs. 2a and 2b, respectively. The steady-state analytical and numerical solutions for the momentum profile and energy distribution are compared, correspondingly, at steady-state time, shown in Figs. 2a and 2b. These results overlap quite well with one another.

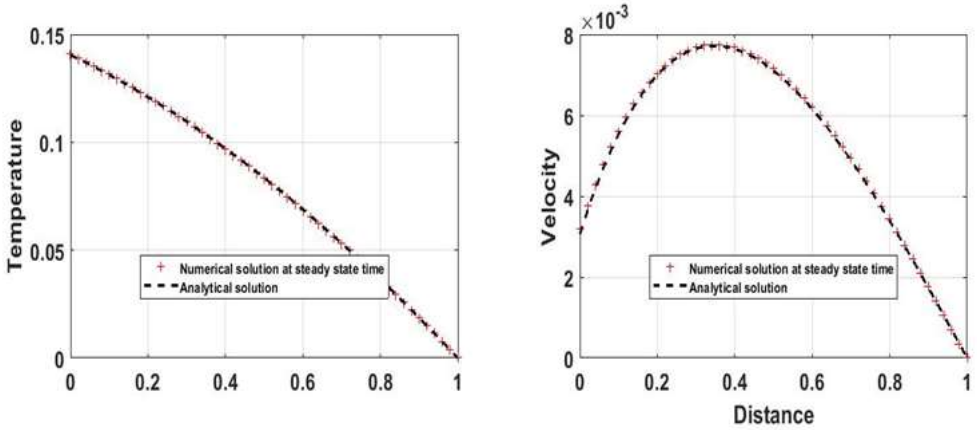

Fig.2.*Correlation between the temperature and velocity profile's transient and steady-state solutions*

6. 2 Dependent Steady-State Solution On Parameters

The graphs in Fig. 3a and 3b show how temperature and velocity vary in response to changes in the local Biot number. More significant Biot numbers suggest more convective heating, which results in improved

flows at lower plates of the energy and momentum profile, which causes the energy and momentum fluid flow to increase. Yet, the fluid surged higher during a biomolecular sort of exothermic reaction. Fig. 4a and 4b's temperature and velocity curves are affected by the chemical process parameter. The energy profile is raised by increasing the chemical components, which is accomplished by increasing the chemical reaction parameter, claims computer research. Only temperature can influence velocity when the parameter is present. As a result, its impact on velocity and temperature are the same. In comparison to Arrhenius and sensitized processes (m=-2 and m=0, respectively), biomolecular reactions (m=0.5) generate greater heat. Fig. 5a and 5b respectively, show how the porous medium has an influence. Fig. 5b shows how the Lorentz force, which is created when the Hartman number is slightly increased, streamlines the momentum boundary layer, slows the flow, and gives the best representation of biomolecular chemical category reactions anytime the Hartman number is increased. Fig. 5a shows an increase in flow rate brought on by an increase in permeability.

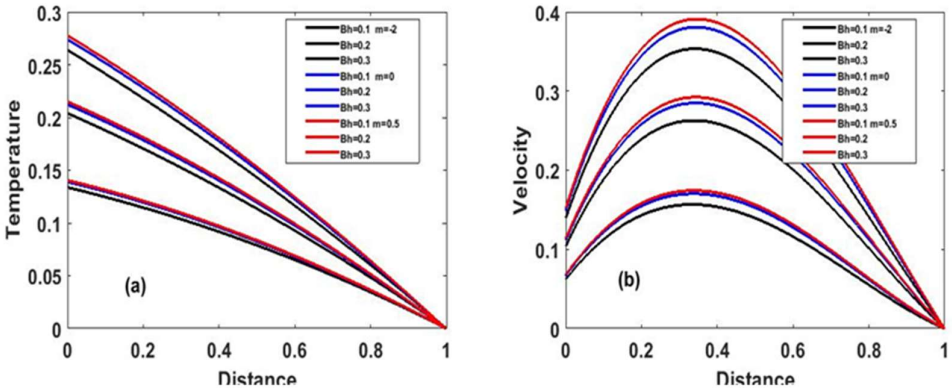

Fig.3. *Impact of Bh on steady-state temperature and velocity circulation*

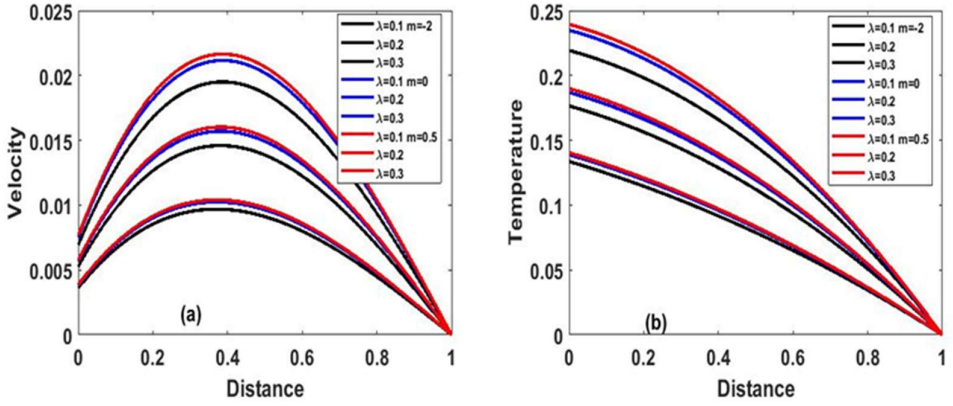

Fig. 4.*Shows the difference between the steady-state temperature and velocity flows for function of* λ .

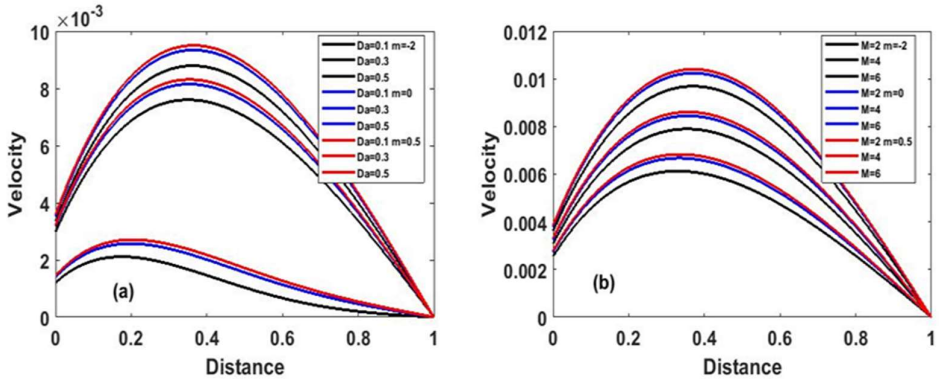

Fig.5.*Deviation from the steady-state velocity field for various Da and Ha values*

6.3 Transient solutions

The following response occurs when the temperature and fluid velocity are both in an unstable condition, as shown in Fig. 6-Fig. 14. According to Hamza's theory [27], Fig. 6a demonstrates that even a slight

increase in Biot number causes a significant increase in the fluid velocity at the bottom surface channel. This is because, although time was identical, flows at lower energy and momentum profile plates improved, indicating that convective heating was more intense. The biomolecular reaction type produces the most significant fluid flow rates regarding energy and momentum profiles. Chemical kinetics is a discipline of physical chemistry that focuses on the reaction rate and the accompanying catalytic mechanism at each stage of the reaction chain. However, it has a wide variety of applications, including molecular reaction dynamics, catalytic dynamics, and element reaction dynamics. Fig. 7a and b show how viscous-reactive fluid characteristics impact velocity and temperature. The temperature and fluid rate in the bottom channel isrising. Momentum and energy fluids improve as the thermostat's strength and quantity of sticky heating source substances grow, resulting in a significant increase in temperature, as reported by Hamza and Abdulsalam [30]. Decreased perceived flow increased fluid velocity, which elevated the temperature.

Additionally, due to the unequal heating of the plates, the temperature rises in the bottom channel while falling in the top track. When the exponent (m = 0.5) was added to the equation, the chemical reaction happened at a higher temperature and velocity. Increases in m cause the chemical reaction source terms in the temperature equation to become stronger, which raises the intensity of those terms. As a result, the temperature of the fluid rises. Parameter m on fluid velocity is minor at best and not as noticeable as the effect of temperature/viscosity coupling.

Fig. 8a and 8b show MHD and porous media impact velocity along a constant, dimensionless time axis. Fig. 8a shows that increased pressure generates the Lorentz force, a drag force that opposes fluid flow and lowers speed. The fluid velocity grows together with the increase in the kinetic exponent m. In general, the flow is entirely hydrodynamic at that point. The fluid's velocity grows as the Darcy number does, as seen in Fig. 8b. By examining the velocity profile over time, this is apparent. Also, it was discovered that fluid velocity rises in proportion to the chemical kinetic exponent m, with the biomolecular process producing the highest velocity profile based on reports by Hamza *et al.* [35]. Fig. 9a and 9b demonstrate that the slip parameter is consistent with steady and unsteady momentum patterns. Because higher values of the slip parameter tend to enhance the response and slipperiness at the lower plate, the velocity at the lower scale increases as the slip parameter increases. At the same time, the fluid momentum continues to increase proportionally to the chemical kinetic exponent type of reaction in Fig. 9b. Fig. 9a demonstrates how the responsiveness and slickness of the lower plate cause the velocity fluid to get stronger as it rises. They may be used in paper mill manufacturing and biomedicine to allow blood to pass through human skin.

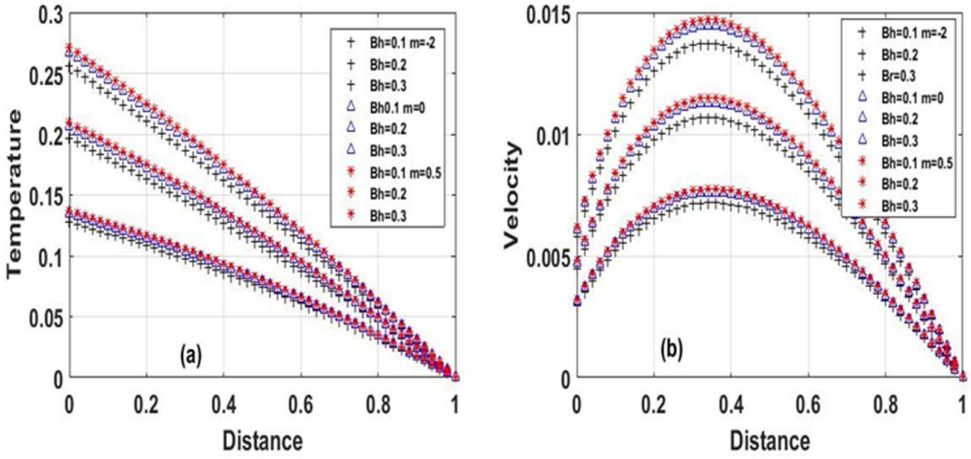

Fig.6. *Deviation from the unsteady state Temperature and Velocity field for various values of* (Bh)

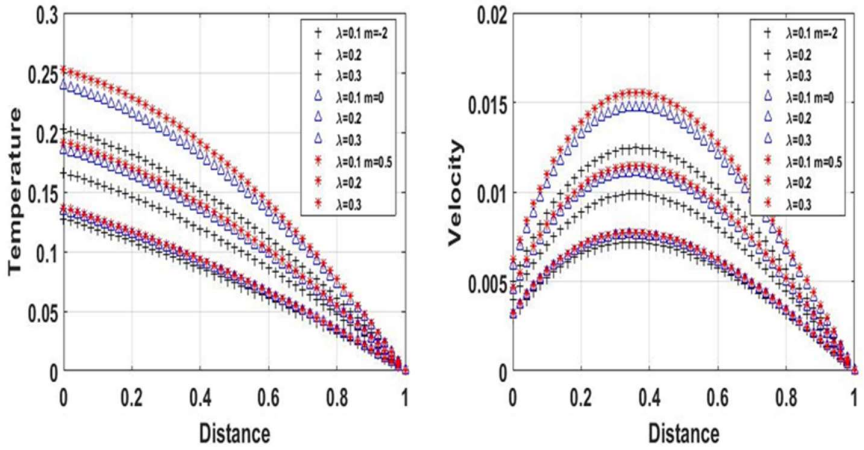

Fig.7. *Deviation from the unsteady state Temperature and Velocity field for various values of* (λ)

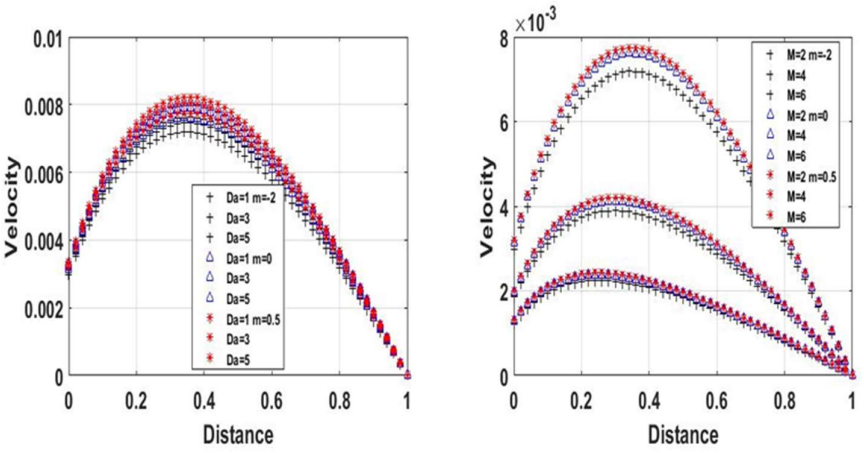

Fig.8. *Deviation from the unsteady velocity field for various values of* (Da) *and* (M)

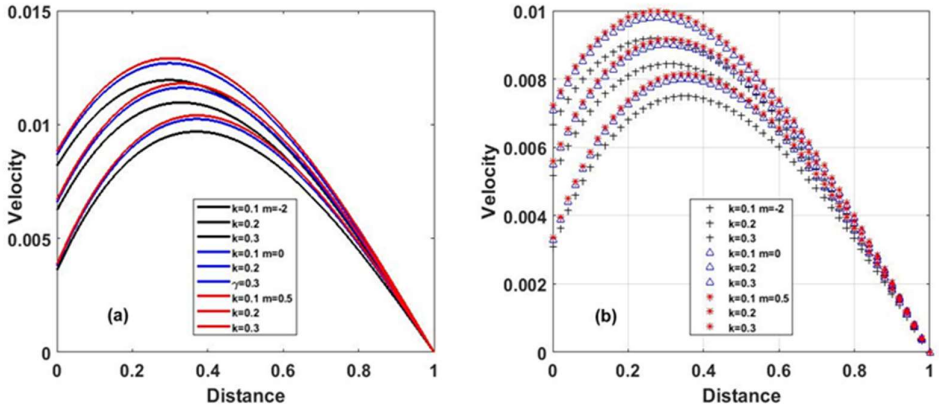

Fig.9. Deviation from the unsteady velocity field for various values of (κ)

6.4 Shear stress and heat transfer rate

Fig. 10a and 10b demonstrate how skin friction may be used to forecast flow characteristics within a wall to a great extent. In Fig. 10a, the bottom plate experiences an increase in skin friction due to convective heating, whereas the top plate has the opposite effect. The chemical reaction patterns shown in Figs. 11a and 11b caused a considerable change in skin friction over time, increasing fluid flow at both plates. Fig. 12a and 12b show two instances of how porous media alter skin friction profiles. Examining the relationship between time and temperature in wall shear stress as time passes, skin friction increases in both the upper and lower channels (t). Fig. 13a and 13b show how MHD affects shear stress. Fig. 13a depicts a significant increase in flow with time and MHD. Because when more Hartmann numbers are

present, the momentum boundary layer along the border of the wall has a better momentum boundary layer. Yet, the fluid flow was reduced on another plate. Fig. 14a and 14b show how skin friction changed over time. Despite the bottom plate's slipperiness, Fig. 14a demonstrates a significant increase in the upper channel shear stress. Fig. 15a and 15b show how the Nusselt number is affected by the local Biot number over time (t). In Figs. 16a and 16b, the Nusselt number difference demonstrated an increase in chemical reaction parameter strength during computational analysis, which increases the heat transfer rate of the chemical composition in both flow channels. We provide Table 1 displays numerical validation for steady and unsteady state velocity and temperature. It is obvious how an unsteady state achieved a steady state. Table 2 compares velocity present work with published work and Table 3 compares Temperature current work and published work.

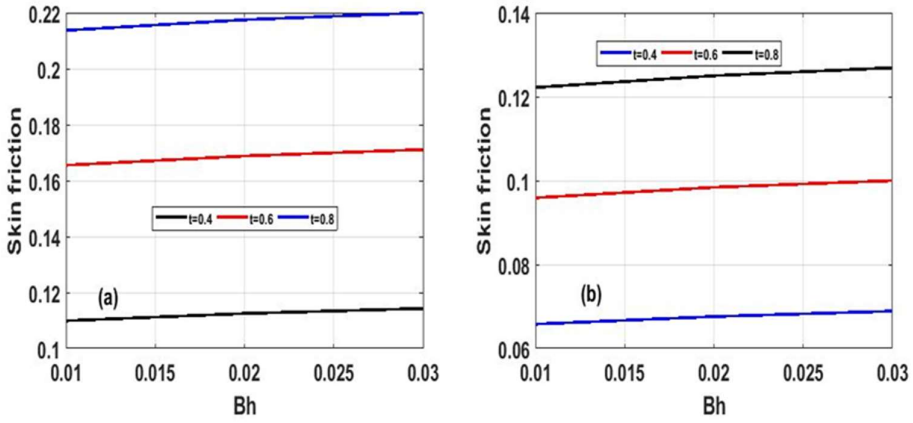

Fig.10. *Shear stress across different* (Bh)

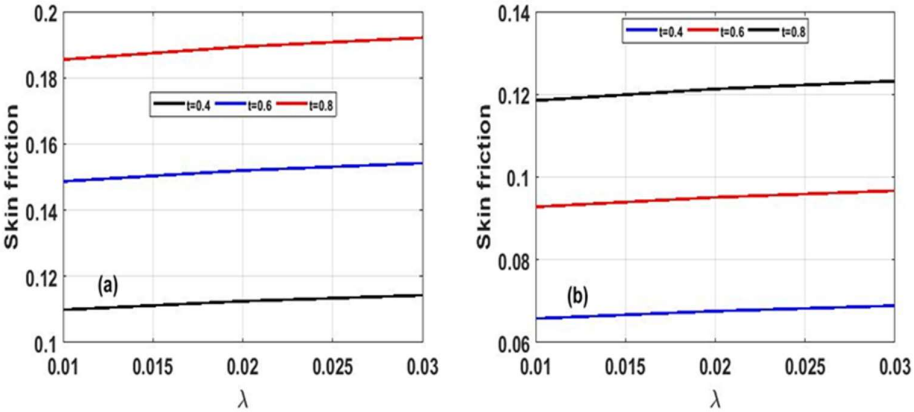

Fig.11. *Shear stress across different* (λ)

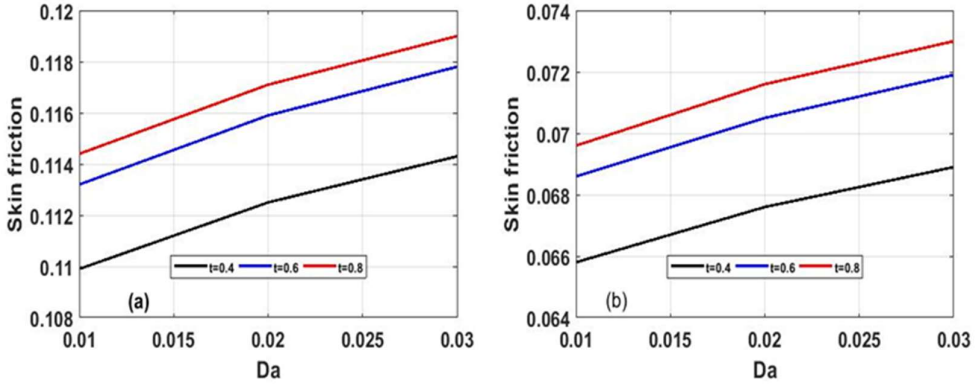

Fig.12. *Shear stress across different* (Da)

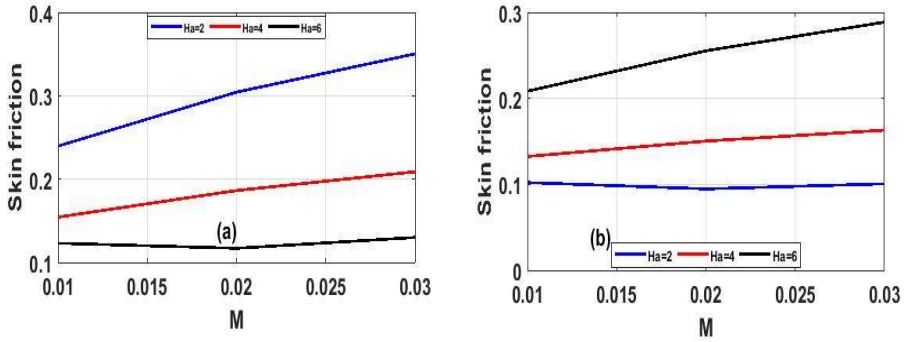

Fig.13. *Shear stress across differen (M)*

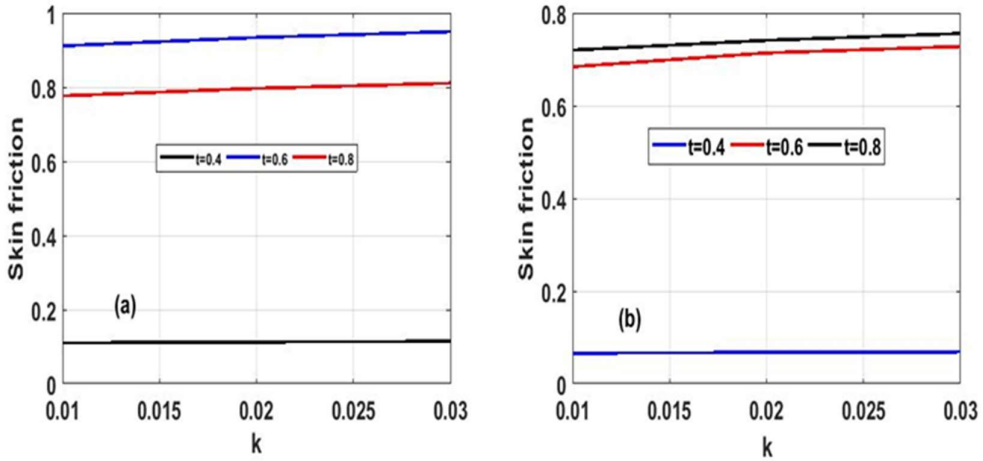

Fig.14. *Shear stress across different* (κ)

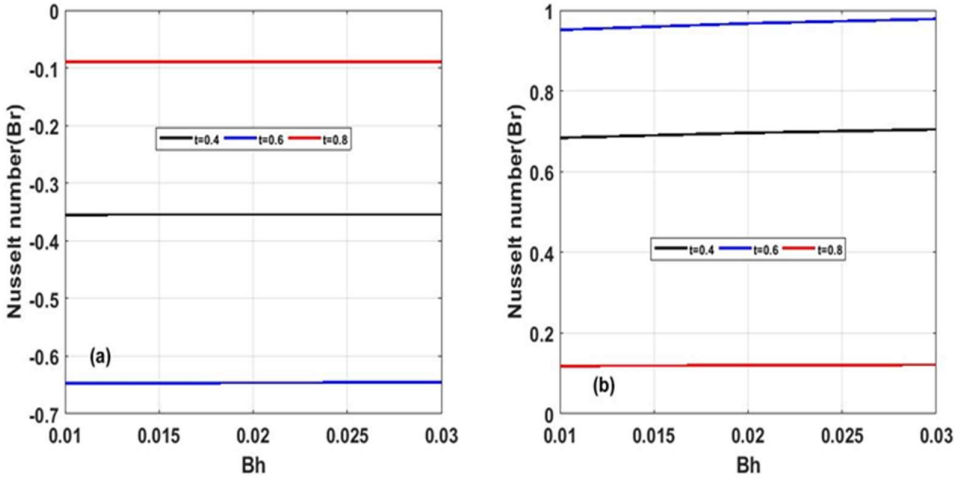

Fig.15.*Heat transfer rate different* (Bh)

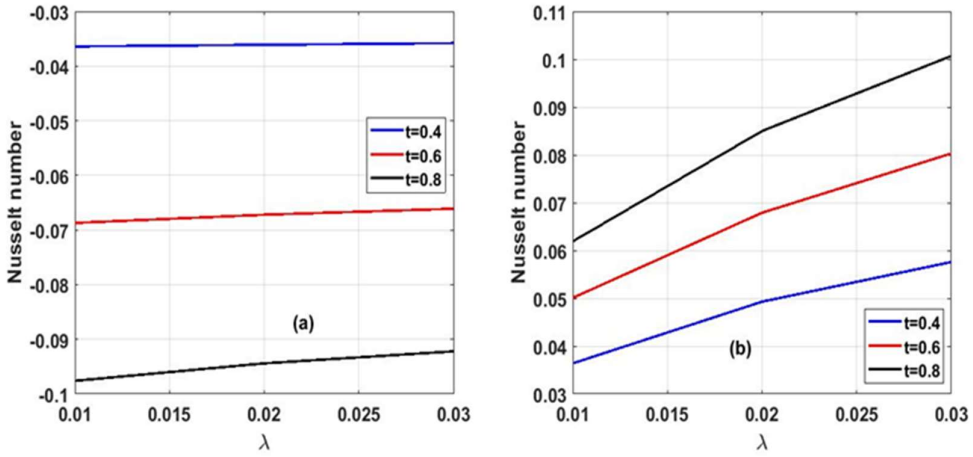

Fig.16. *Heat transfer rate across different* (λ)

6. 5 Validation

Table 1.*Shows numerical validation for Steady and Unsteady state velocity and temperature*

Steady-state Velocity $U(m)$	**Unsteady state Velocity** $U(m)\ \Delta t = 0.020$	**Steady-state Temperature** $T(m)$	**Unsteady state Temperature** $T(m)\ \Delta t = 0.020$
0.3198	0.3278	0.0290	0.0287
0.2823	0.2884	0.0225	0.0252
0.2439	0.2484	0.0220	0.0217
0.2047	0.2079	0.0184	0.0182
0.1649	0.1669	0.0148	0.0146
0.1245	0.1255	0.0112	0.0110
0.0835	0.0838	0.0075	0.0074
0.0420	0.0420	0.0038	0.0037

Table 2.*Shows a comparison of velocity present work and published work*
$Ha = 0, m = 0, Bh = 0.1, \kappa = 0.1, Da = 100000, \lambda = 0.1$

(m)	**Hamza [27]** $U(m)$	**Present** work $U(m)$
0.1	1.1557	1.1557
0.3	1.3056	1.3057
0.5	1.4557	1.4557
0.7	1.6057	1.6057
0.9	1.7557	1.7557

Table3. **Shows a comparison of Temperature present work and published work**
$m = 0, Bh = 0.1, \lambda = 0.1$

(m)	**Hamza [27]** $\phi(m)$	**Present** work $\phi(m)$
0.1	0.7323	0.7323
0.3	0.7280	0.7281
0.5	0.7155	0.7155
0.7	0.7073	0.7073
0.9	0.6991	0.6991

7. Advantages and disadvantages

Advantages

- This method obtains a solution providing a comprehensive analysis of the fluid flow through the porous medium between two vertical walls due to buoyance forces, convective heating, and Lorentz forces.
- The study provides insight into the impact of flow parameters on the fluid and the spike in momentum and energy profile, contributing to a better understanding of the system

Disadvantages

- There is less study on the effects of other flow such as velocity and temperature in the chemical process to understand the study of impact on temperature and velocity gradients.
- The steady and unsteady flow must be further analyzed to get a deeper understanding of the system's behavior.

8. Conclusions

In this paper, it is explored how steady and erratic chemical kinetic exponents affect the free convective slip flow of hydromagnetic in a vertical channel filled with porous media. The tests were built around the idea of Boussinesq. Convective heating of the lower channel and the fluid's reactive nature are what ignite the flow. Moreover, dimensionless equations for momentum, energy, and boundary conditions in a transient state were solved using the implicit finite difference scheme approach. Nonetheless, the steady-state governing equation was approached via homotopy perturbation.

Moreover, the impacts of flow parameters on the fluid were examined, and the findings produced by the numerical approach were compared to those obtained by the analytical technique, with good agreement observed. Furthermore, the validation of the numerical solution coincides with the previous literature. During the computation, the chemical reaction parameter, chemical kinetic exponent, thermal Biot number, porous medium, and Navier slip parameter were shown to be highly reliant on the spike in momentum and energy profile. Similarly, it was demonstrated throughout the computational process that increasing MHD increases the thickness of the momentum boundary layer, resulting in a dropin fluid velocity following Hamza et al. [6]. From a physical standpoint, M = 0 signifies no magnetic impact, and the flow is entirely hydrodynamic. This is expected since applying a transverse magnetic field always results in a resistance-type force known as the Lorentz force.

Additionally, as the Darcy number grows, so does the fluid's velocity, as shown in the velocity profile. When there is no porous material, the channel gap is occupied by the primary atom that built up the structure of the solid. Still, the porous medium has different uses, such as water purification, gas separation, and thermal conductivity, which may be utilized. Moreover, the skin friction and heat transfer rate regarding the Nusselt number were examined. It was discovered that increasing the porous medium, chemical reaction parameter, thermal Biot number, and slippery slip parameter at the bottom plate enhanced skin friction while decreasing it at the top plate

Compliance with Ethical Standards

Conflicts of interest: Authors declared that they have no conflict of interest.

Human participants: The conducted research follows the ethical standards and the authors ensured that they have not conducted any studies with human participants or animals.

References

[1] A. J. Chamkha, “Mixed convection flow along a vertical permeable plate embedded in a porous medium in the presence of a transverse magnetic field,” Numerical Heat Transfer, Part A: Applications: An International Journal of Computation and Methodology, vol. 34, no. 1, pp. 93–103, 2007.

[2] Y. Joshi and B. Gebhart, “Mixed convection in porous media adjacent to a vertical uniform heat flux surface", International Journal of Heat and Mass Transfer, vol. 28, no. 9, pp. 1783– 1786, 1985.

[3] A. Chamkha, R.S. R. Gorla and K. Ghodeswar, “Non-similar solution for natural convective boundary layer flow over a sphere embedded in a porous medium saturated with a nanofluid,” Transport in Porous Media, vol. 86, no. 1, pp. 13–22, 2011.

[4] Y. Mahmoodi, K. Hooman and K. Vafai,"Convective Heat Transfer in Porous Media (New York, U.S.A.: Taylor & Francis Group", LLC CRC Press,2020.
[5] M. Veerakrisha, G. Subba Reddy and A. J.Chamkha,"Hall effect on unsteady MHD oscillatory free convection flow of second-grade fluid through the porous medium between two vertical plates", Physics of Fluids, Vol. 30, pp. 023106,2018.
[6] M. M.Hamza, A. Shuaibu andA. S. Kamba, "Unsteady MHD free convection flow of an exothermic fluid in a convectively heated vertical channel filled with porous medium",Sci Rep12, pp. 11989, 2022.
[7] A. Wakif, A. Chamkha, T.Thumma, I.L.Animasaunand R.Sehaqui,"Thermal radiation and surface roughness effects on the thermo-magneto-hydrodynamic stability of alumina–copper oxide hybrid nanofluids utilizing the generalized Buongiorno's nanofluid model",Journal of Thermal Analysis and Calorimetry, Vol. 143 no. 2, pp. 1201 – 1220, 2021.
[8] H. M. Shawky, "Magnetohydrodynamic Casson fluid flow with heat and mass transfer through a porous medium over a stretching sheet", J. Porous Media, Vol. 15, pp. 393–401,2012.
[9] R.Cortell, "MHD flow and mass transfer of an electrically conducting fluid of second grade in a porous medium over a stretching sheet with chemically reactive species", Int. J. Heat MassTransf, Vol.49, pp. 1851–1856, 2006.
[10] S. Nadeem, R. U.Haq, N. S. Akbar, Z.H. Khan, "MHD three-dimensional Casson fluid flow past a porous linearly stretching sheet", Alexandria Eng. J. Vol. 52, pp. 577–582, 2013
[11] R. P. Harshad, "Thermal radiation effects on MHD flow with heat and mass transfer of micropolar fluid between two vertical walls", International Journal of ambient energy. Vol. 42, no. 11, pp. 1281-1296, 2021a.
[12] R. P. Harshad, "Cross-diffusion and heat generation effects on mixed convection stagnation point MHD carreau fluid in a porous medium", International Journal of ambient energy. Vol. 42, no. 11, pp. 1281-1296, 2021b.
[13] R.N. Jat, G. Chand, D. Rajotia, "MHD heat and mass transfer for viscous flow over nonlinearly stretching sheet in a porous medium", Therm. Energy Power Eng., Vol. 3, pp. 191–197, 2014.
[14] A.Khalid, I.Khan, A.Khan and S. Shafie, "Unsteady MHD free convection flow of Casson fluid past over an oscillating vertical plate embedded in a porous medium", Eng. Sci. Technol. Int. J. Vol. 80, pp. 1–9, 2015.
[15] I. S.Oyelakin, S. Mondal and P. Sibanda, "Unsteady Casson nanofluid flow over a stretching sheet with thermal radiation, convective and slip boundary conditions", *Alexandria*Eng. J.,Vol. **55**, pp. 1025–1035,2016.
[16] K. Bhattacharyya and G. C. Layek, "Slip Effect on Diffusion of Chemically Reactive Species in Boundary Layer Flow over a Vertical Stretching Sheet with Suction or Blowing",Chem. Eng. Commun.Vol.198, pp. 1354–1365, 2011.
[17] M.Shen, F. Wang and Chen,"H. MHD mixed convection slip flow near a stagnation-point on a nonlinearly vertical stretching sheet",Bound. Value Probl.,Vol. 78, 2015.
[18] K.Bhattacharyya, S. Mukhopadhyay and G. C.Layek, "Slip effects on an unsteady boundary layer stagnation-point flow and heat transfer towards a stretching sheet",Chinese Phys. Lett., Vol.28, pp. 094702, 2011.
[19]A.Ishak, N. A. Yacob and N. Bachok, "Radiation effects on the thermal boundary layer flow over a moving plate with convective boundary condition",Meccanica, Vol.46, pp. 795–801, 2011.
[20] Kurma,"Radiation Effect on magnetohydrodynamics flow with induced magnetic field and Newtonian Heating/Cooling," Propulsion and Power Research,Vol.1-11, 2021.
[21] Reddy and Sademaki, "A numerical study on the Newtonian heating effect on heat absorbing MHD Casson flow of dissipative fluid past an oscillating vertical porous plate",International Journal of Mathematics and Mathematical Sciences, Vol. 1, pp. 1-16, 2022.
[22] D. Kumar, A.K. Singh, "Effect of Newtonian heating/cooling on hydromagnetic free convection in alternate conducting vertical concentric annuli", in Applications of Fluid Dynamics, Lecture Notes in Mechanical Engineering, 2017.
[23] S. Chaudhary, K.M. Kanika, M.K. Choudhary, "Newtonian heating and convective boundary condition on MHD stagnation point flow past a stretching sheet with viscous dissipation and Joule heating", Indian J. Pure Appl. Phys., Vol. 56, pp. 931e940, 2018.
[24] S. K. Ahmad, S. Abdulsalam and M.M. Hamza,"Free Convection Slip Flow with Diffusion- Thermo in a Convectively Heated Vertical Porous Channel",Journal of Applied Physical Science International,Vol. 8 no. 2, pp. 58-71, 2017.
[25] K. Gangadhar, D.V. Kumar, A.J. Chamkha, T. Kannan and G. Sakthivel, "Effects of Newtonian heating and thermal radiation on micropolar ferrofluid flow past a stretching surface: spectral quasi-linearization method", Heat Transfer-Asian Res. Vol. 49,no. 2, pp. 838e857, 2020.
[26] A. J. Chamkha,"Hartmann Newtonian radiating MHD flow for a rotating vertical porous channel immersed in a Darcian Porous Regime: An exact solution",International Journal of Numerical Methods for Heat & Fluid Flow, Vol.24,no. 7, pp. 1454 – 1470.
[27] M. M. Hamza,"Free convection slip flow of an exothermic fluid in a convectively heated vertical channel",Ain shams Engineering Journal,Vol. 9, pp. 1313-1323, 2018.
[28] M. M. Hamza, M.Z. Shehu and B.H. Tambuwal,"Steady state MHD free convection slip flow of an exothermic fluid in a convectively heated vertical channel",Saudi Journal of Engineering Technology, Vol.6 no. 10,pp. 364-370, 2021.
[29] G. Mahanta and S. Shaw,"3D Casson fluid flows past a porous linearly stretching sheet with convective boundary condition",Alexandria Eng. J.(2021), Vol.54, pp. 653–659,2015.
[30] M. M. Hamza and S. Abdulsalam, "Influence of chemical kinetic exponent on transient mixed convective hydromagnetic flow in a vertical channel with convective boundary condition," International Journal of Thermofluids, vol. 16, article 100220, 2022.

[31] S. Nadeem, R. U. Haq and N. S. Akbar, “MHD three-dimensional boundary layer flow of Casson nanofluid past a linearly stretching sheet with convective boundary condition”,IEEE Trans. Nanotechnol., Vol.13, pp. 1326–1332, 2014.
[32] S. U.Jan, S. U.Haq, S. I. A. Shah and I. Khan, “Heat and mass transfer of free convection flow over a vertical plate with chemical reaction under wall-slip effect”,Arab. J. Sci. Eng. Vol. 44 no. 12, pp. 9869–9887,2019.
[33] A. R. Bestman, “Radiative heat transfer to flow of a combustible mixture in a vertical pipe,” International Journal of EnergyResearch, vol. 15, no. 3, pp. 179–184, 1991.
[34] M. A. Alabraba, A. R. Bestman and A. Ogulu, “Laminar convection in binary mixture of hydromagnetic flow with radiative heat transfer, I,” Astrophysics and Space Science, vol. 195, no. 2, pp. 431–439, 1992.
[35] M. M. Hamza, S. Abdulsalam and S. K. Ahmad, "Time-Dependent Magnetohydrodynamic (MHD) Flow of an Exothermic Arrhenius Fluid in a Vertical Channel with Convective Boundary Condition," Advances in Mathematical Physics, vol. 2023, Article ID 7173925, 13 pages, 2023.

Nomenclature

g	acceleration due to gravity	R	universal gas constant
Pr	Prandtl number	θ_T	ambient temperature
H	dimensionless distance between the plates	k	thermal conductivity of the fluid
t'	dimensional time	E	activation energy
t	dimensionless time	h	heat transfer coefficient
T'	the dimensional temperature of the fluid	**Greek letters**	
T_0'	the initial temperature of the fluid and plates	β	volumetric coefficient of thermal expansion
C_0'	the initial concentration of the fluid and channel	λ	Frank- Kamenetskii parameter
u	the dimensional velocity of the fluid	ϕ	dimensionless temperature
U	the dimensionless speed of the fluid	ρ	density of the fluid
C_p	specific heat of the liquid at constant pressure	ε	activation energy parameter
C_0^*	the initial concentration of the reactant species	κ	dimensionless slip velocity
x'	dimensional coordinate parallel to the plate's	ν	kinematic viscosity
y'	dimensional coordinate perpendicular to the plate		
y	dimensional coordinate perpendicular to the plate		

Appendix

$$D_1=(1+m\varepsilon),\quad D_2=(m-1)\varepsilon,\quad D_3=\frac{m}{2}(m-1)\varepsilon^2,\quad D_4=(\frac{v_0}{6}m^3+\frac{v_1}{2}m^2)$$

$$D_5=(\frac{v_0^2}{24}m^4+\frac{2v_0v_1}{12}m^3+\frac{v_1^2}{4}m^3),\qquad D_6=(\frac{v_0^2}{12}m^4+\frac{2v_0v_1}{6}m^3+\frac{v_1^2}{2}m^2)$$

$$D_7=(\frac{v_0^2}{12}m^4+\frac{2v_0v_1}{6}m^3+\frac{v_1^2}{2}m^2),\qquad D_8=(\frac{v_0}{120}m^5+\frac{v_1}{24}m^4)$$

$$D_9=(\frac{v_7}{6}m^3+\frac{v_8}{2}m^2),\ D_{10}=(\frac{A}{24}m^4+\frac{v_0}{6}m^3+\frac{v_1}{2}m^2)$$

$$D_{11}=(\frac{v_0}{120}m^5+\frac{v_1}{24}m^4),D_{12}=(\frac{v_0^2}{720}m^6+\frac{2v_0v_1}{240}m^5+\frac{v_1^2}{48}m^4),$$

$$D_{13}=(\frac{v_0^2}{360}m^6+\frac{2v_0v_1}{120}m^5+\frac{v_1^2}{24}m^4),\quad D_{14}=(\frac{v_0^2}{360}m^6+\frac{2v_0v_1}{120}m^5+\frac{v_1^2}{24}m^4),$$

$$D_{16}=(\frac{v_2}{6}m^3+\frac{v_3}{2}m^2),\ D_{17}=(\frac{v_0}{120}+\frac{v_1}{24}),\qquad D_{18}=(\frac{A}{24}+\frac{v_6}{6}+\frac{v_7}{2})$$

$$D_{19}=(\frac{v_0}{120}+\frac{v_1}{24}),\qquad D_{20}=(\frac{v_0^2}{720}+\frac{2v_0v_1}{240}+\frac{v_1^2}{48}),$$

$$D_{21}=(\frac{v_0^2}{360}+\frac{2v_0v_1}{120}+\frac{v_1^{2\,4}}{24}),\qquad D_{22}=(\frac{v_0^2}{360}+\frac{2v_0v_1}{120}+\frac{v_1^2}{24}),$$

$$D_{23}=(\frac{v_2}{6}+\frac{v_3}{2}),$$

$$v_1=\frac{Bh\theta a}{Bh+1},\qquad v_0=-v_1,\qquad v_2=Bhv_{3,}\qquad v_3=\frac{\lambda(\frac{1}{2}+D_1D_4+D_5+D_2D_6+D_3D_6)}{(Bh+1)}$$

$$v_7=\frac{Gre(\frac{v_0}{6}+\frac{v_1}{2})-\frac{A}{2}}{(1+\Gamma)},\qquad v_8=\Gamma v_7,\qquad v_{10}=\Gamma v_9$$

$$v_9=\frac{1}{(1+\Gamma)}\left(Ha\left[-GreD_{19}+\frac{v_7}{6}+\frac{v_8}{2}\right]-Gre\left[-\lambda(\frac{1}{24}+D_1D_{24}+D_{20}+D_2D_{21}+D_3D_{22})+D_{23}\right]\right)$$